Synthesis, Structure, and Properties of PBO/SWNT Composites[&]

Satish Kumar,*,† Thuy D. Dang,‡ Fred E. Arnold,‡ Arup R. Bhattacharyya,† Byung G. Min,†,# Xiefei Zhang,† Richard A. Vaia,‡ Cheol Park,§ W. Wade Adams,⊥ Robert H. Hauge,⊥ Richard E. Smalley,⊥ Sivarajan Ramesh,⊥ and Peter A. Willis⊥

School of Textile and Fiber Engineering, Georgia Institute of Technology, Atlanta, Georgia 30332-0295, Air Force Research Laboratory, WPAFB, Ohio 45433-7750, ICASE/NASA Langley Research Center, Mail Stop 226, Hampton, Virginia 23681-2199, and Center for Nanoscale Science and Technology, Rice University, Houston, Texas 77005

Received March 29, 2002; Revised Manuscript Received August 6, 2002

ABSTRACT: Poly(*p*-phenylene benzobisoxazole) (PBO) has been synthesized in the presence of single-wall carbon nanotubes (SWNTs) in poly(phosphoric acid) (PPA) using typical PBO polymerization conditions. PBO and PBO/SWNT lyotropic liquid crystalline solutions in PPA have been spun into fibers using dry-jet wet spinning. The tensile strength of the PBO/SWNT fiber containing 10 wt % SWNTs is about 50% higher than that of the control PBO fibers containing no SWNTs. The structure and morphology of these fibers have been studied.

Introduction

PBO (Figure 1a), a rigid-rod polymer, is characterized by high tensile strength, high stiffness, and high thermal stability.[1−3] Mechanical and electrical properties of SWNTs[4] (Figure 1b) are predicted to be quite extraordinary.[5−9] The single-wall carbon nanotube diameter is reported to vary from 0.4 to above ∼3 nm.[9] To take advantage of the extraordinary mechanical, electrical, and thermal properties of carbon nanotubes, several studies have been reported where attempts have been made to reinforce polymer and other matrix systems with carbon nanotubes. These studies include pitch/SWNT composite fiber,[10] polystyrene/MWNT (multiwall carbon nanotubes),[11] PMMA/SWNT,[12] and polypropylene/nanocarbon fiber.[13] While these studies confirm the potential benefits of reinforcing polymer and other matrices with carbon nanotubes, the challenge is to achieve good SWNT dispersion in the polymer and other matrices at significant nanotube weight fractions. In this paper we report PBO synthesis in poly(phosphoric acid) (PPA) in the presence of SWNTs, where SWNTs are well-dispersed, and the results of PBO/SWNT fiber processing as well as structure−property studies.

Experimental Methods

The liquid crystalline solutions are prepared by the in-situ polycondensation of bis(aminothiophenol) or bis(aminophenol) as their dihydrochlorides and aromatic diacid monomers in the presence of SWNTs. The in-situ polymerizations are carried out in PPA to give polymer or the polymer/SWNT concentrations of 14 wt %, which forms an anisotropic reaction mixture. SWNT concentrations were 0, 5, and 10 wt % with respect to the polymer concentration utilized in the polymerization. SWNTs used in this study had an average diameter of ∼0.95 nm and were produced from the high-pressure carbon monoxide (HiPco) process developed at Rice University.[14,15] As an example, a description of the polymerization scheme of PBO/SWNT (95/5) is given below.

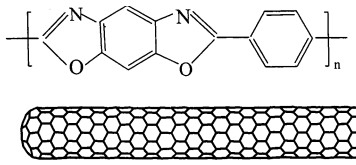

Figure 1. Structure of (a, top) PBO and (b, bottom) SWNT.

Into a 250 mL glass flask, equipped with a mechanical stirrer and a nitrogen inlet/outlet, were placed 4.2612 g (0.02 mol) of 1,4-diaminoresorcinol dihydrochloride, 4.0605 g (0.02 mol) of terephthaloyl chloride, and 12.14 g of phosphoric acid (85%). The resulting mixture was dehydrochlorinated under a nitrogen atmosphere at 65 °C for 16 h and subsequently at 80 °C for 4 h. At this stage, 0.234 g of purified[16] and vacuum-dried HiPco nanotubes was added to the reaction flask. The mixture was heated to 100 °C for 16 h while stirring and then cooled to room temperature. P_2O_5 (8.04 g) was added to the mixture to generate poly(phosphoric acid) (77% P_2O_5). The mixture was stirred for 2 h at 80 °C and then cooled to room temperature. Further P_2O_5 (7.15 g) was then added to the mixture to bring the P_2O_5 concentration to 83% and the polymer concentration to 14 wt %. The mixture was heated at 160 °C for 16 h with constant stirring. Stir opalescence was observed during this step. The mixture was finally heated to 190 °C for an additional 4 h while stirring. An aliquot of the polymer solution (generally referred to as dope) was precipitated, washed in water, and dried under vacuum at 100 °C for 24 h. An intrinsic viscosity of 14 dL/g was determined in methanesulfonic acid at 30 °C.

A control polymerization of pure PBO was also carried out under the same conditions without adding SWNTs. For PBO/SWNT (90/10) composition, 0.47 g of purified HiPco tubes (SWNT) was added to the mixture. The sequence of steps and polymerization conditions remain the same as those for PBO/SWNT (95/5) composition. Intrinsic viscosity values of PBO and PBO/SWNT (90/10) were 12 and 14 dL/g, respectively.

PBO and PBO/SWNT fibers were dry-jet wet spun using a piston driven spinning system manufactured by Bradford University Research Ltd. Polymer dope preheated to 50 °C was transferred under a dry nitrogen atmosphere to the spinning cylinder and was heated to 100 °C for about 5 h before spinning. A 50 μm stainless steel filter (from Anderson Wire

* Corresponding author: e-mail satish.kumar@textiles.gatech.edu.
† Georgia Institute of Technology.
‡ Air Force Research Laboratory.
§ ICASE/NASA Langley Research Center.
⊥ Rice University.
Current address: School of Adv. Materials and System Engineering, Kumoh National University of Technology, Kumi, Korea 730-701.

[&] This paper is dedicated to Dr. Fred E. Arnold for his 36 years of service to the Air Force Research Laboratory.

10.1021/ma0205055 CCC: $22.00
Published on Web 10/05/2002

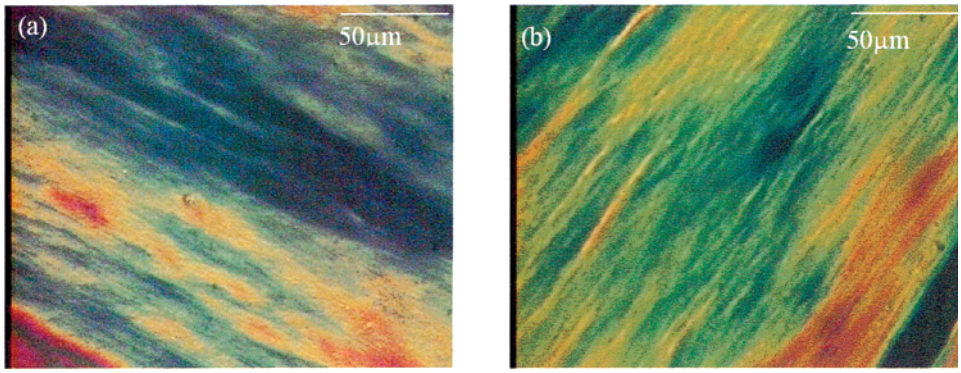

Figure 2. Crossed-polarized optical micrographs of (a) 14 wt % PBO in PPA and (b) 14 wt % PBO/SWNT (90/10) in PPA.

Table 1. Mechanical Properties of PBO and PBO/SWNT Composite Fibers

sample	fiber diameter (μm)	tensile modulus (GPa)	strain to failure (%)	tensile strength (GPa)	compressive strength (GPa)
PBO	22 ± 2	138 ± 20	2.0 ± 0.2	2.6 ± 0.3	0.35 ± 0.6
PBO/SWNT (95/5)	25 ± 2	156 ± 20	2.3 ± 0.3	3.2 ± 0.3	0.40 ± 0.6
PBO/SWNT (90/10)	25 ± 2	167 ±15	2.8 ± 0.3	4.2 ± 0.5	0.50 ± 0.6

Works, Inc.) was used in line for fiber spinning, and the spinneret diameter was 250 μm. PBO and PBO/SWNT (95/5) fibers were spun at 100 °C, while PBO/SWNT (90/10) was spun at 150 °C. The fiber exited into a 10 cm long air gap before entering a distilled water coagulation bath maintained at room temperature. Draw ratios as high as 10 were achieved. Fibers were wound on a plastic spool, washed in running water for a week, and subsequently dried overnight in a vacuum at 80 °C. Dried fibers were heat-treated at 40 MPa tension in nitrogen at 400 °C for 2 min using a Thermolyne 21100 tube furnace.

Optical microscopy on the PBO and PBO/SWNT dopes was carried out on a Leitz polarizing microscope. Thermogravimetric studies were conducted at 10 °C/min using a TA Instruments TGA 2950. Fiber shrinkage and creep studies were carried out using a TA Instruments TMA 2940. For tensile testing, fibers were mounted on cardboard tabs. Testing was performed on an Instron universal tensile tester (model 5567) using 2.54 cm gage length at a strain rate of 2%/min. About 20 samples were tested in each case. Fiber diameters were measured using laser diffraction. Wide-angle X-ray diffraction was performed on a multifilament bundle on a rotating anode X-ray generator (RU-200BH, Rigaku-Rotaflex, 20 kV, 50 mA) with Cu Kα radiation (λ = 0.154 nm) using a Statton camera. Patterns were collected on Kodak stage-phosphor screens and read using a Molecular Dynamics Storm 820 image plate reader.

Raman spectra were taken using an Almega dispersive visible Raman spectrometer (Thermo Nicolet). A 785 nm incident light excitation was used, and the laser beam was focused on the fiber samples using an optical microscope (Olympus BX50) with a 50× objective lens. A low (10%) laser excitation power was maintained to minimize sample heating, which often results in a spectral downshift. A reference spectrum was monitored throughout the entire experiment and Raman shift caused by heating was negligible. A 25 μm slit was used as an aperture to collect the 180° backscattered radiation through the microscope.

Results and Discussion

Figure 2 shows optical micrographs of PBO and PBO/SWNT (90/10) dope under crossed polarizers. No aggregates are observed in the PBO/SWNT dope, suggesting good SWNT dispersion at the optical scale during PBO polymerization conditions. By comparison, optical microscopy of melt-blended PP/SWNT showed distinct SWNT aggregates.[17]

The mechanical properties of heat-treated PBO and PBO/SWNT composite fibers are given in Table 1, and typical stress−strain curves are shown in Figure 3. The modulus data have not been corrected for instrumental compliance, which means that the actual modulus value is higher than the measured value.[18] It is also well-known that the tensile strength can exhibit significant gage length dependence,[18] and the data in Table 1 have been obtained at only one gage length (2.54 cm), which means that the tensile strength at shorter gage lengths is expected to be higher. The data in Table 1 show that tensile modulus, tensile strength, and elongation to break of PBO/SWNT (90/10) fiber are higher than the values for the control PBO fiber by approximately 20, 60, and 40%, respectively. The higher tensile strength of the fiber containing SWNT is qualitatively consistent with the higher tensile strength predictions for SWNT as compared to PBO. Several PBO and PBO/SWNT spinning and heat-treatment trials were conducted. Average PBO tensile strength values for these trials varied between 1.8 and 2.6 GPa, and that for the PBO/SWNT (90/10) fibers varied between 2.9 and 4.2 GPa. Thus, for various trials a tensile strength increase of 40−60% was obtained by incorporating 10 wt % SWNT in PBO. The tensile strength of the commercial PBO fiber (Zylon HM) is 5.8 GPa.[19] If similar tensile strength improvement with the incorporation of SWNTs is achieved in Zylon, then it should result in a fiber with a tensile strength above 8 GPa.

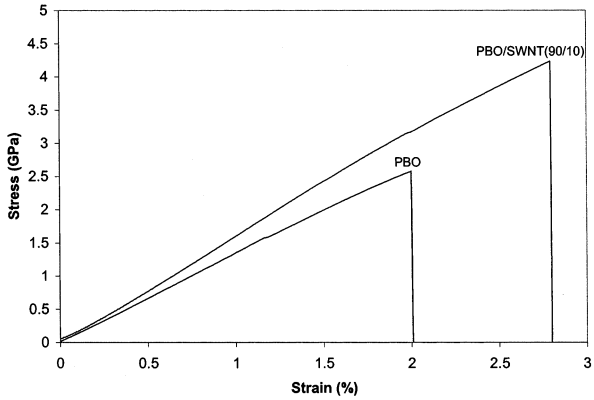

Figure 3. Typical stress−strain curves for PBO and PBO/SWNT (90/10) fibers.

Work of rupture per unit volume, as measured by area under the stress−strain curve, for the PBO and PBO/

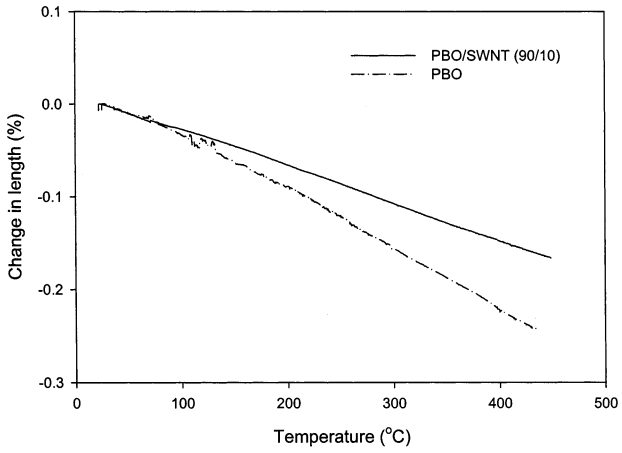

Figure 4. Thermal shrinkage at 25 MPa stress in PBO and PBO/SWNT (90/10) when heated at 10 °C/min in nitrogen.

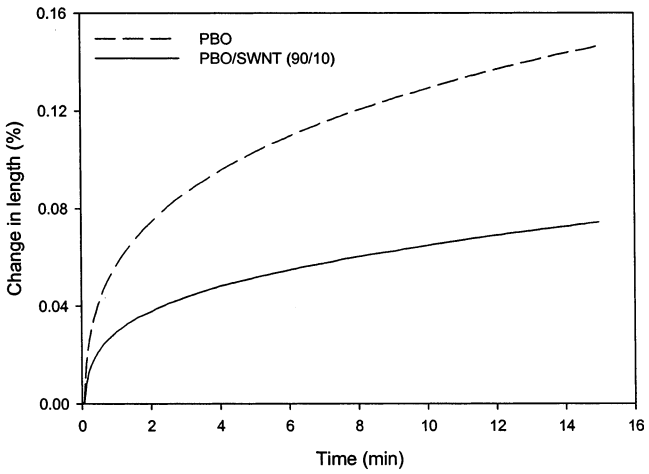

Figure 5. Creep behavior of PBO and PBO/SWNT (90/10) fibers at 400 °C at a stress of 250 MPa.

SWNT (90/10) fibers was 22 and 53 MPa, respectively. Compressive strength, measured using recoil test,[20] shows moderate improvement with the addition of SWNTs. This is consistent with the previous reports suggesting that the addition of inorganic whiskers[21] and carbon nanotubes[13] can improve fiber compressive strength. The coefficient of thermal expansion (CTE) obtained from the data in Figure 4 for PBO and PBO/SWNT (90/10) fiber is −6 and −4 ppm/°C, respectively. PBO/SWNT (90/10) also exhibit reduced creep at 400 °C as compared to the control PBO fiber (Figure 5). Thermal degradation behavior of PBO/SWNT (90/10) in nitrogen (Figure 6) as well as in air (not shown) is comparable to that of the pure PBO fiber. For comparison, thermal degradation behavior of SWNTs is also plotted in Figure 6.

X-ray diffraction of PBO/SWNT fibers up to 10 wt % SWNT is essentially the same as that for the control PBO fiber (Figure 7). The full width at half-maximum values for the azimuthal scans (not shown) of the (100) reflection[22] in PBO and PBO /SWNTs (90/10) composite fibers were both 15°, indicating identical PBO orientation in the two. X-ray diffraction studies were done on a multifilament bundle. Single-filament studies using synchrotron radiation will enable more accurate determination of orientation and structural parameters to determine any subtle influence of the SWNT on the structure and organization of PBO crystalline regions and fibrillar structure.

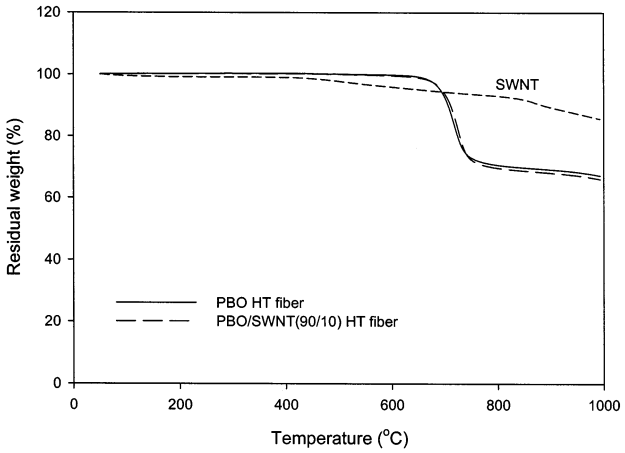

Figure 6. Weight loss in PBO, PBO/SWNT (90/10), and SWNT when heated at 20 °C/min in nitrogen.

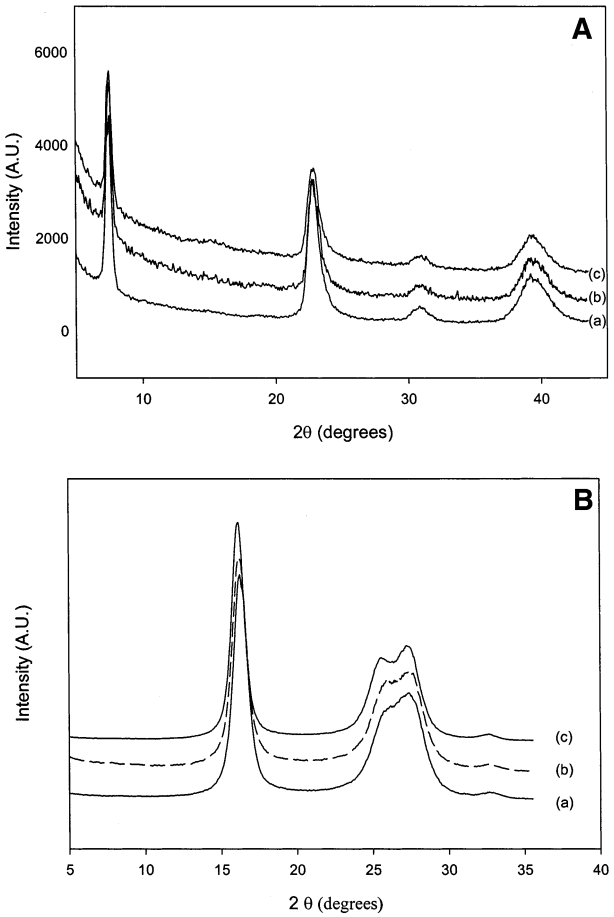

Figure 7. Wide-angle X-ray diffraction: (A) meridional and (B) equatorial scans of (a) PBO, (b) PBO/SWNT (95/5), and (c) PBO/SWNT (90/10) composite fibers.

Rigid-rod polymeric fibers such as PBO and poly(*p*-phenylene benzobisthiazole) (PBZT) are fibrillar.[23] Transverse fibril dimensions in the 7−10 nm range have been reported in PBZT.[24] Likewise, SWNTs assemble into "ropes" of about 10 nm diameter.[25] The term "rope" used by the carbon nanotube community represents a similar structural assembly as the term "fibril" used by the polymer and fiber community. From extensive scanning electron microscopic examination (SEM photographs not shown) of PBO and PBO/SWNT composite fibers, it was not possible to say whether any given fibril contained only PBO molecules, SWNT molecules, or both.

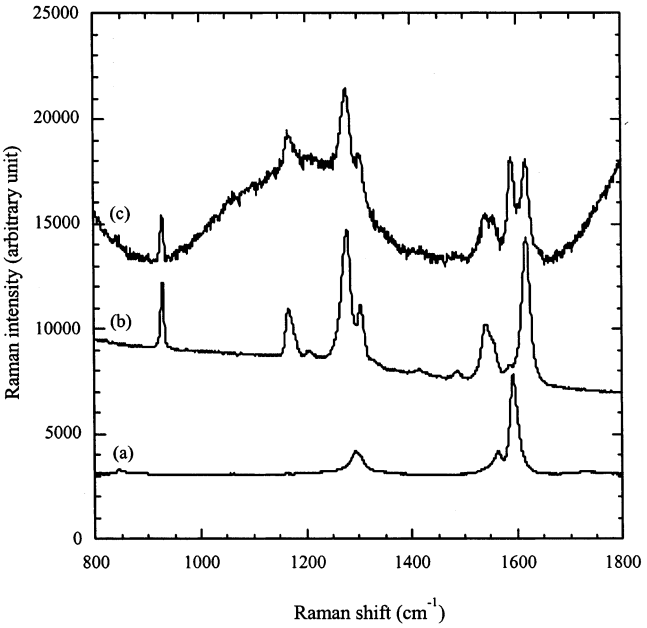

Figure 8. Raman spectra of (a) SWNT, (b) Zylon HM (PBO), and (c) PBO/SWNT (90/10) fibers.

The dc electrical conductivity, measured by four-probe method, of both PBO and PBO/SWNT (90/10) fibers was below the resolution limit of the instrument: $\sim 1 \times 10^{-11}$ S/m. It is reported for other systems that the percolation threshold for tubes with large aspect ratios aligned along the fiber axis is ~20 vol %.[26,27] On the other hand, for solution-spun polyamide 11 fibers containing intrinsically conducting polyaniline, the critical concentration for percolation was only 5 wt %, and conductivity increased with increasing fiber draw ratio.[28] Authors attributed this to phase separation, forming fibril-like channels of polyaniline in polyamide 11, resulting in a low percolation threshold. The fact that 10 wt % SWNT did not significantly increase the dc conductivity suggests they are well-dispersed and highly aligned. If SWNTs were slightly misaligned or aggregated into clusters with some finite structure orthogonal to the fiber axis, a low percolation threshold should be observed.

Raman spectra of the HiPco SWNT, PBO (Zylon HM), and PBO/SWNT (90/10) fibers are given in Figure 8. The tangential mode of the pristine SWNT was observed at 1592 cm^{-1}. The vibration mode of the backbone *p*-phenylene ring was observed in PBO[29] as a strong peak at 1618 cm^{-1} along with prominent peaks at 929, 1168, 1207, 1279, 1304, 1414, 1485, and 1541 cm^{-1}. The discernible tangential mode peak of SWNT at 1590 cm^{-1} as well as the characteristic PBO peaks at 928, 1167, 1276, 1302, 1537, and 1618 cm^{-1} were detected in the heat-treated PBO/SWNT (90/10) fiber, superimposed over strong fluorescence. The characteristic breathing mode of the SWNT at around 200−300 cm^{-1} was buried in the strong fluorescence. The PBO fiber spun under the same conditions exhibited strong fluorescence masking the characteristic PBO peaks. Therefore, the commercial PBO fiber (Zylon HM) Raman spectra was used for comparison.

Conclusions

SWNTs were well-dispersed during PBO synthesis in PPA. PBO/SWNT composite fibers have been successfully spun from the liquid crystalline solutions using dry-jet wet spinning. The addition of 10 wt % SWNT increased PBO fiber tensile strength by about 50% and reduced shrinkage and high-temperature creep. The existence of SWNT in the spun PBO/SWNT fibers was evidenced by the 1590 cm^{-1} Raman peak.

Acknowledgment. The authors acknowledge the help of T. V. Sreekumar and David Tomlin for scanning electron microscopy, Gary Price for X-ray diffraction, and Max Alexander for electrical conductivity experiments. Financial support for this research from the Air Force Office of Scientific Research and support at Rice University in developing the HiPco process from NASA, the Office of Naval Research, the Texas Advanced Technology Program, and the Robert A. Welch Foundation is gratefully acknowledged.

Note Added after ASAP Posting

This article was released ASAP on 10/5/2002. A revised version was posted on 10/28/2002 with a dedication on page 1 and Figure 2 in color on page 2.

References and Notes

(1) Adams, W. W., Eby, R. K., McLemore, D. E., Eds.; *The Materials Science and Engineering of Rigid-Rod Polymers*; Materials Research Society Symp. Proc.: Pittsburgh, PA, 1989; Vol. 134.
(2) Kumar, S. In *International Encyclopedia of Composites*; Lee, S. M., Ed.; VCH: New York, 1991; Vol. 4, p 51.
(3) Kuroki, T.; Tanaka, Y.; Hokudoh, T.; Yabuki, K. *J. Appl. Polym. Sci.* **1997**, *65*, 1031.
(4) Iijima, S. *Nature (London)* **1991**, *354*, 56.
(5) Yakobson, B. I.; Smalley, R. E. *Am. Sci.* **1997**, *85*, 324.
(6) Treacy, M. M. J.; Ebbesen, T. W.; Gibson, J. M. *Nature (London)* **1996**, *381*, 678.
(7) Wong, E. W.; Sheehan, P. E.; Lieber, C. M. *Science* **1997**, *277*, 1971.
(8) Poncharal, P.; Wang, Z. L.; Ugarte, D.; de Heer, W. A. *Science* **1999**, *283*, 1513.
(9) Baughman, R. H.; Zakhidov, A. A. de Heer, W. A. *Science* **2002**, *297*, 787.
(10) Andrews, R.; Jacques, D.; Rao, A. M.; Rantell, T.; Derbyshire, F.; Chen, Y.; Chen, J.; Haddon, R. C. *Appl. Phys. Lett.* **1999**, *75*, 1329.
(11) Quin, D.; Dickey, E. C.; Andrews, R.; Rantell, T. *Appl. Phys. Lett.* **2000**, *76*, 20.
(12) Haggenmueller, R.; Gommans, H. H.; Rinzler, A. G.; Fischer, J. E.; Winey, K. I. *Chem. Phys. Lett.* **2000**, *330*, 219.
(13) Kumar, S.; Doshi, H.; Srinivasrao, M.; Park, J. O.; Schiraldi, D. A. *Polymer* **2002**, *43*, 1701.
(14) Nikolaev, P.; Bronikowski, M. J.; Bradley, R. K.; Rohmund, F.; Colbert, D. T.; Smith, K. A.; Smalley, R. E. *Chem. Phys. Lett.* **1999**, *313*, 91.
(15) Bronikowski, M. J.; Willis, P. A.; Colbert, D. T.; Smith, K. A.; Smalley, R. E. *J. Vac. Sci. Technol.* **2001**, *19*, 18000.
(16) Chiang, I. W.; Brinson, B. E.; Huang, A. Y.; Willis, P. A.; Bronikowski, M. J.; Margrave, J. L.; Smalley, R. E.; Hauge, R. H. *J. Phys. Chem.* **2001**, *105*, 8297. As received, HiPco tubes were treated at 250 °C in moist air for over 15 h, and then impurities were continuously removed using the Soxhlet extraction set up with 20.2% hydrochloric acid. After Soxhlet extraction, TGA in air showed 0.63 wt % residue. This corresponded to 0.4 wt % FeO based on iron oxide that was identified by the XPS analysis.
(17) Sreekumar, T. V.; Bhattacharyya, A. R.; Kumar, S.; Ericson, L. M.; Smalley, R. E., submitted to *Polymer*.
(18) Sahafeyan, M.; Kumar, S. *J. Appl. Polym. Sci.* **1995**, *56*, 517.
(19) Kitagawa, T.; Ishitobi, M.; Yabuki, K. *J. Polym. Sci., Polym. Phys. Ed.* **2000**, *38*, 1605.
(20) Kozey, V. V.; Jiang, H.; Mehta, V. R.; Kumar, S. *J. Mater. Res.* **1995**, *10*, 1044.
(21) Harmer, M. A.; Phillips, B. R. U.S. Patent No. 5,512,368, April 30, 1996.

(22) Takahashi, Y. *Macromolecules* **1999**, *32*, 4010.
(23) Krause, S. J.; Haddock, T. B.; Vezie, D. L.; Lenhert, P. G.; Hwang, W. F.; Price, G. E.; Helminiak, T. E.; Obrien, J. F.; Adams, W. W. *Polymer* **1988**, *29*, 1354.
(24) Cohen, Y.; Thomas, E. L. *Macromolecules* **1988**, *21*, 433, 435.
(25) Figure 1B in: Liu, J.; Rinzler, A. G.; Dai, H.; Hafner, J. H.; Bradley, R. K.; Boul, P. J.; Lu, A.; Iverson, T.; Shelimov, K.; Huffman, C. B.; Rofriguez-Macias, F.; Shon, Y.-S.; Lee, T. R.; Colbert, D. T.; Smalley, R. E. *Science* **1998**, *280*, 1253.
(26) Munson-McGee, S. H. *Phys. Rev. B* **1991**, *43*, 3331.
(27) Taya, M.; Kim, W. J.; Ono, K. *Mech. Mater.* **1998**, *28*, 53.
(28) Zhang, Q.; Jin, H.; Wang, X.; Jing, X. *Synth. Met.* **2001**, *123*, 481.
(29) Kitagawa, T.; Yabuki, K.; Young, R. J. *Polymer* **2001**, *42*, 2101.

MA0205055